JOURNAL OF OPTOELECTRONICS AND ADVANCED MATERIALS, Vol. 11, No. 9, September 2009, p. 1064 - 1071

Determination of the hydrogenated amorphous silicon density of states parameters from photoconductivity measurements♣

C. LONGEAUD*, J. A. SCHMIDT[a], R. R. KOROPECKI[a], J. P. KLEIDER
Laboratoire de Génie Electrique de Paris, UMR 8507 CNRS, Universités Paris VI et XI, 11 rue Joliot-Curie, Plateau de Moulon, 91190 Gif sur Yvette, France.
[a] *INTEC (UNL-CONICET) and FIQ (UNL), Güemes 3450, S3000GLN Santa Fe, Argentina.*

In this paper, after a short recall of the information that can be extracted from different experiments based on the photoconductivity properties of a semiconductor, we present experimental results obtained on a thin film of hydrogenated amorphous silicon in the as-deposited, light-soaked and annealed states. We show that, taking advantage of the apparent discrepancies between the results of dc photoconductivity and modulated photoconductivity, density of states distributions as well as some of their capture coefficients can be deduced. The evolution of these quantities with light-soaking and annealing is also shown. The experimental results are also illustrated by means of numerical simulations.

(Received November 5, 2008; accepted December 15, 2008)

Keywords: Thin films, Photoconductivity, Computer simulation

1. Introduction

Many of the experiments designed to investigate the electronic transport parameters and densities of states (DOS) of semiconductors are based on their photoconductive properties. Among these, the simplest one is the steady state photoconductivity (SSPC), for which a dc light flux is shone onto the sample. More sophisticated is the modulated photocurrent (MPC) technique, in which the dc flux is modulated and the resulting ac current recorded to give a DOS spectroscopy [1-4]. However, none of these experiments is self sufficient, since, to take the example of the MPC, fundamental parameters like the capture cross sections of the gap states, are difficult to derive when MPC is used alone. In this paper, we first recall briefly the theoretical background of these experiments, by means of a short presentation of the basic equations of each technique, and show that even the SSPC technique can reveal information on the material DOS [5-6]. In section 3, we present experimental results obtained on hydrogenated amorphous silicon (a-Si:H), either in the as-deposited, light-soaked or annealed states, and a-Si:H DOS parameters extracted from these data will be proposed.

Finally, we illustrate the complementarity of these three experiments – and of our experimental results – by means of a numerical simulation.

2. Theoretical presentation

We shall not recall all the calculations since they have already been presented in other papers [3-7]. We shall present the basic equations and the final results instead. Considering a semiconductor containing m species of monovalent states in the band gap, characterized by their capture coefficients C_n^i and C_p^i for electrons and holes respectively ($1 \le i \le m$), the continuity and charge neutrality equations are:

$$\frac{\partial n}{\partial t} = G - \sum_1^m \int_{E_v}^{E_c} \left(C_n^i n^i \left[1 - f^i \right] - e_n^i f^i \right) N^i dE \,, \tag{1}$$

$$\frac{\partial p}{\partial t} = G - \sum_1^m \int_{E_v}^{E_c} \left(C_p^i p^i f^i - e_p^i \left[1 - f^i \right] \right) N^i dE \,, \tag{2}$$

$$\frac{\partial f^i}{\partial t} = C_n^i n + e_p^i - f^i \left[C_n^i n + C_p^i p + e_n^i + e_p^i \right], \tag{3}$$

$$0 = \left\{ p - p_0 - (n - n_0) - \sum_1^m \int_{E_v}^{E_c} N^i \left(f^i - f_0 \right) dE \right\}, \tag{4}$$

♣ Paper presented at the International School on Condensed Matter Physics, Varna, Bulgaria, September 2008

To write these equations, we have assumed that the sample is in a coplanar geometry in between two ohmic contacts, biased with a dc voltage and uniformly illuminated by a flux of light generating carriers by band to band transitions. We have also assumed that the exchange of carriers in localised states occurs mainly by multiple trapping, i.e. hopping between defect states is neglected. The electron (hole) concentration in the extended states is labelled n (p), n_0 (p_0) being the concentration under dark equilibrium, the superscript ^{i} denotes the i^{th} species of trap, e_n^i (e_p^i) is the energy-dependent emission rates of electrons (holes) , G is the band-to-band generation rate from the valence band below E_v to the conduction band above E_c, N^i is the energy-dependent density of states, f^i is the occupation function under illumination, and f_0 is the occupation function under dark equilibrium.

All the experiments described in this paper are based on the superposition of a dc flux and a small perturbation that could be a step function (SSPC) or a small modulation (MPC). Therefore, we can write most of the quantities of Eqs. (1-4) as $Q=Q_0+\delta Q$.

2.1. DC photoconductivity

It is well known that the photoconductivity σ_{ph} is usually found proportional to the generation rate G raised to the power γ, $\sigma_{ph} \propto G^{\gamma}$. In the following, we shall assume that electrons are the majority carriers, but all the development would be valid assuming that holes were the majority carriers. We have already shown that some information on the density of states is contained in γ, and an expression for it was given, assuming that δQ is a small step function [5]. From this expression, a relation between the transport parameters and the experimental data was proposed:

$$\frac{N(E_{fn})C_n}{\mu_n} = \frac{qG}{k_B T \sigma_{ph}}\left[\frac{1}{\gamma} - 1\right], \qquad (5)$$

in which T is the temperature, k_B the Boltzmann constant, q the absolute value of the electron charge, μ_n the extended states mobility, and C_n the capture coefficient of the *dominant recombination centre* and NOT necessarily the capture coefficient of the states located around the quasi Fermi level E_{fn}, $N(E_{fn})$. The energy position can be calculated from the photoconductivity value σ_{ph} by:

$$E_c - E_{fn} = k_B T \ln\left[\frac{q\mu_n N_c}{\sigma_{ph}}\right], \qquad (6)$$

where N_C is the effective DOS at E_c.

It should be noted that the quantity NC/μ in Eq. (5) is fully determined from known experimental data. Of course, Eq. (5) is only valid in the case $\gamma < 1$, that is in a regime for which the recombination path is well defined. Indeed, in some materials it is observed that, keeping the same dc flux, a temperature variation causes for instance a quenching of the photoconductivity in a-Si:H [8, 9] or a sudden change of the lifetime in 'sensitizable' crystals (e.g. CdS) [10]. These phenomena can be attributed to a change in the main recombination path from one type of state to another, with very different capture cross sections.

Finally, a proper energy scaling from Eq. (6) requires the knowledge of $\mu_n N_c$.

2.2. AC photoconductivity

In this case, the small perturbation is a modulation of the applied dc flux, the total flux shone onto the sample being $F = F_{dc}+F_{ac}\sin(\omega t)$, and the experiment based on such an illumination is named modulated photocurrent (MPC). Two regimes have been widely studied: a regime for which the sample response is linked to recombination processes and a regime linked to trapping and release processes. Basically, it was shown that the first regime occurs when ω is low, at least lower than the emission rate from the quasi Fermi level of the majority carriers, $e_n(E_{fn})$ [4]. For this reason, we shall name it low frequency MPC (MPC-LF). The second regime occurs in the opposite case, that is when $\omega >> e_n(E_{fn})$, and is called high frequency MPC (MPC-HF).

A link between the MPC-LF and the dc photoconductivity measurements was previously underlined, showing that the ac data measured at low frequency could be used to calculate the γ value [5]. Indeed, in dc, one has:

$$\frac{\delta\sigma_{ph}}{\sigma_{ph}} = \gamma\frac{\delta G}{G} \quad , \qquad (7)$$

by logarithmic differentiation of the relationship between σ_{ph} and G, and in ac, one has:

$$\frac{|\sigma_{ac}|}{\sigma_{ph}} = \gamma\frac{G_{ac}}{G} \quad , \qquad (8)$$

in which $|\sigma_{ac}|$ and G_{ac} are the ac photoconductivity modulus and the amplitude of the ac generation rate, respectively. These expressions show that, though apparently very different, the MPC and dc photoconductivity experiments are intimately linked. A more refined treatment of the MPC-LF data also leads to an estimate of the DOS at E_{fn} by the relation:

$$N(E_{fn}) = \frac{2G}{k_B T}\frac{\tan(\phi)}{\omega} \quad , \qquad (9)$$

ϕ being the phase shift of the ac current referred to the excitation, and the energy scaling being achieved according to Eq. (6).

The second regime of the MPC experiment was widely studied and exemplified [1-4], and it was shown that the NC/μ value can be deduced from:

$$\frac{N(E_\omega)C_n}{\mu_n} = \frac{2qG_{ac}}{\pi k_B T}\frac{\sin\phi}{|\sigma_{ac}|} \quad , \qquad (10)$$

the energy of the probed states, E_ω, being given by:

$$E_c - E_\omega = k_B T \ln\left(\frac{C_n N_c}{\omega}\right) \quad . \qquad (11)$$

The capture coefficient, C_n, involved in Eq. (10) is that of the probed states located at E_ω. It can also be seen that, as for the photoconductivity experiment, NC/μ values are fully determined from experimental data. However, a proper energy scaling requires the knowledge of C_nN_c.

In summary, dc photoconductivity measurements provide an estimate of NC/μ, C being the capture coefficient of the main recombination states and N the DOS at the quasi Fermi level. The MPC-LF, the results of which can also be treated as the photoconductivity data, gives information on the DOS at E_{fn}. The MPC-HF provides an estimate of NC/μ, N being the DOS at an energy level, depending on ω and C, the capture coefficient of these states. Another difference between the MPC-LF and MPC-HF is the link between the DOS parameters and the energy scaling. For the first technique, the energy scaling depends on μ_nN_c, and on C_nN_c for the second. Performing these three experiments on the same sample – and adjusting N, C and μ to match the different results – should lead not only to a better knowledge of N, but also of some of the capture cross sections of the different states present in the gap, and even of the extended states mobility.

3. Experimental results

These three experiments have been performed on various thin films of a-Si:H [6]. We lack space to present all these results, and we shall concentrate on a single sample. This film was prepared in a radio frequency powered plasma enhanced chemical vapour deposition (rf-PECVD) reactor, at a substrate temperature of 423 K, from a mixture of hydrogen and silane (97 % H_2, 3% SiH_4), at high pressure (1.4 Torr) and high rf power (110 mW/cm^2). These deposition conditions lead to a material called polymorphous silicon [11]. The film was annealed at 450 K under vacuum (10^{-5} Torr) for a few hours, before measurements (as-deposited or in the AD state). Accelerated light-soaking of the sample was achieved under 300 mW/cm^2 red light at 80 °C (light-soaked or LS state), the evolution of the photocurrent being monitored to check the saturation. The annealing of the film was performed at 450 K over 12 hours under vacuum (annealed or ANN state). The three experiments exposed in Section 2 were performed on this film, in each of the states (AD, LS and ANN).

For all three experiments, the light was provided by a set of 9 light emitting diodes with a peak wavelength at 650 nm. The dc photoconductivity measurements were performed in the temperature range $100 \le T \le 450$ K in 10 K steps, with eight different fluxes ranging from 1.5×10^{13} to 3.0×10^{15} cm^{-2}s^{-1} in a 1-2-5 scale ($1\times1.5\times10^{13}$, $2\times1.5\times10^{13}$, $5\times1.5\times10^{13}$ cm^{-2}s^{-1}, …). The γ values were calculated according to Eq. (7) with two different fluxes: F and $1.2\times F$ (i. e. $\delta F = 0.2\times F$). For the highest fluxes, ac measurements were also performed, σ_{ac} being recorded with an ac flux of the order of 20 % of the dc flux (i. e. $F_{ac} = 0.2\times F$) and using Eq. (8) to calculate γ.

The MPC-LF was performed with a high dc flux of 3.0×10^{15} cm^{-2}s^{-1}, in the same temperature range as the photoconductivity, in 10 K steps, with an ac flux of 20 % the dc one. The frequencies of the modulation were in the range 1-300 Hz. The maximum temperature was limited to 390 K, to avoid annealing during the experiment. The density of states at the quasi Fermi level was calculated by taking the first slope of tan(Φ) vs ω for the very first values of low ω. However, for some temperatures, it happens that this slope was negative due to a negative phase shift (the phase lead regime). Hence, for these temperatures, we have also used the first *positive* slope of tan(Φ) vs ω (the phase lag regime) to calculate the density of states.

The MPC-HF was performed with a dc flux of 10^{13} cm^{-2}s^{-1}, the ac flux being some 20 % of the dc one. The frequencies of the modulation were in the range 12 Hz – 40 kHz, and the temperature varied between 120 K and 450 K in 30 K steps.

We present in Fig. 1 the NC/μ values determined from γ measurements, or γ-NC/μ, performed under ac and dc illuminations. As predicted by our theoretical developments, the curves agree rather well, showing that there is definitely a link between the dc photoconductivity and the MPC-LF experiments. It can also be seen that there is a gap in the curves between 0.3 and 0.4 eV, corresponding to γ values larger than one, from which the γ-NC/μ data cannot be calculated.

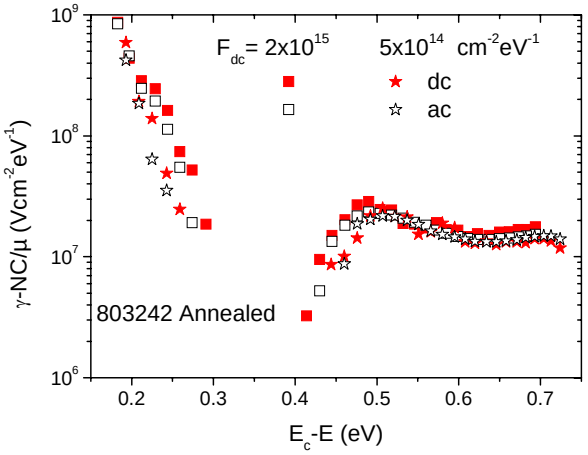

Fig. 1. γ-NC/μ calculated from photoconductivity measurements performed in dc (full symbols) and ac (open symbols) for two different fluxes.

We display in Figs 2-4 the results of the different experiments applied to the sample in the AD, LS and ANN states, respectively.

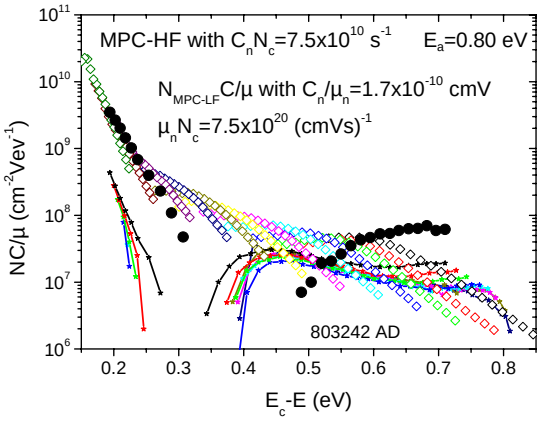

Fig. 2. NC/μ vs energy determined from MPC-HF (Open diamonds), MPC-LF (full circles) and γ measurements (full line+stars) on the AD film.

We have to recall that the MPC-HF *NC/μ* is made of different sets of points obtained at different frequencies, one set for each temperature. The data obtained at high frequencies result in a superimposition of the different sets, and it is this upper envelope that represents the 'true' MPC-HF *NC/μ*. The origin of the 'tails' below this envelope has been discussed elsewhere [4] and we shall not return to this point.

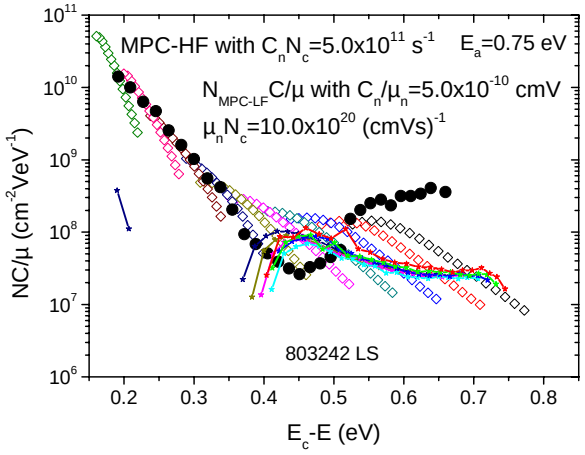

Fig. 3. NC/μ vs energy determined from MPC-HF (Open diamonds), MPC-LF (full circles) and γ measurements (full line+stars) on the LS film.

In each figure, the values of the capture coefficient and of the extended states mobility have been adjusted to obtain a good match between the *NC/μ* calculated from the MPC-LF and the MPC-HF data for the conduction band tail (CBT) states. Indeed, due to its exponential increase, it is likely that at low energies the CBT states, probed at low temperatures, are the main dominant states as far as the MPC is concerned, and that is why MPC-HF and MPC-LF should give the same *NC/μ*.

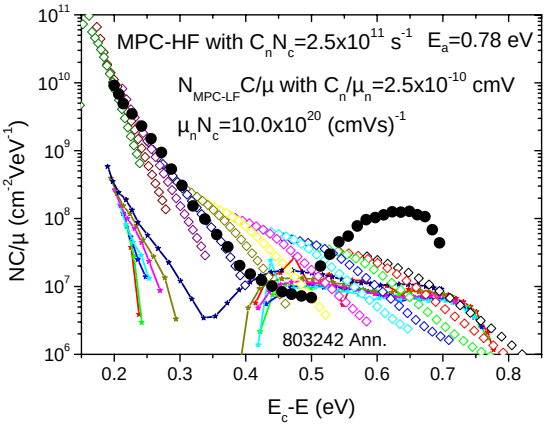

Fig. 4. NC/μ vs energy, determined from MPC-HF (Open diamonds), MPC-LF (full circles) and γ measurements (full line+stars) on the ANN film.

This match is done on the horizontal axis by adjusting the energy scaling, since this is achieved following two different equations [Eqs. (6) and (11)] in which the two quantities C_nN_c and μ_nN_c are involved. On the vertical axis, the product $N\times C_n/\mu_n - N$, being determined by the MPC-LF experiment is adjusted to the *NC/μ* directly calculated from the MPC-HF data. The values of the ratio C_n/μ_n and of the product μ_nN_c to achieve this matching are displayed in the figures.

This matching gives orders of magnitude of the extended states mobility, choosing for N_c the same value as for crystalline silicon (c-Si), and of the electron capture coefficient of the band tail. However, since the *γ-NC/μ* has been plotted with the same energy scaling as for the MPC-LF, one can see that there is a large discrepancy (a factor of ~ 10) between the *NC/μ*'s calculated from MPC-HF and *γ-NC/μ* in the CBT region. This behaviour is linked to the fact that the *C* is certainly not the same: in MPC-HF the *C* is that of the probed states. In photoconductivity, the *C* is that of the main recombination states. At the low temperatures at which the experiments are performed to probe the CBT, it is highly probable that only two types of state are involved in the recombination process, the CBT and the valence band tail (VBT). Therefore, it is likely that the *C* involved in the *γ-NC/μ* is the electron capture coefficient of the VBT states, and thus the ratio C_n^{VBT}/C_n^{CBT} can be estimated.

As far as the deeper states are concerned, they are probed at higher temperatures, and it is clear from Figs 2-4 that the parameters chosen to achieve a good match between MPC-HF and MPC-LF in the CBT region are not convenient at all. This is simply due to the fact that the

electron capture coefficient of the deep states may be completely different from that of the CBT.

For instance, if one bears in mind that the MPC-HF gives NC/μ values and that the MPC-LF gives N values alone, it means that the C of the CBT used to plot the NC/μ from the MPC-LF data is probably too high. Thus, slightly above the dark Fermi level (the position of which is given by the activation energies E_a displayed in the figures), the defect distribution presents a rather high density with a rather low capture cross-section. Indeed, to set back the MPC-LF NC/μ to the MPC-HF NC/μ values, one should choose a C between 5 to 10 times lower than the C of the CBT states (C_n^{CBT}). Note also that the deep state density increases with light-soaking, an indication that these states are probably dangling bonds (DB), whose density depends on hydrogen bonding as described by the defect pool model [12].

We can also compare the γ-NC/μ values and the MPC-HF NC/μ values found in the same energy region. It can be seen that close to the Fermi level, there is a rather good agreement between these values. In a previous paper, we have shown [5] that the ratio between γ-NC/μ and MPC-HF-NC/μ values is of the same order as the ratio between the neutral DB and positive DB electron capture coefficients (C_n^{DB0} and C_n^{DB+}, respectively). Thus, our results indicate that these two coefficients are not very different, giving $C_n^{DB0} / C_n^{DB+} \approx 0.25 - 1$.

The most difficult energy range to extract information about is located between the CBT states and the DB states. Indeed, this region corresponds to measurement temperatures leading to γ values larger than one. Thus, Eq. (5) is no longer valid. In this temperature range, we observe a quenching of the photoconductivity, corresponding to a transition of the main recombination path from the deep states towards the VBT states. Note that in almost the same temperature range, we have obtained negative values of tan(ϕ) for the lowest frequencies of the MPC-LF experiment. This is why in the energy range 0.3-0.45 eV we observe a gap for both γ-NC/μ and MPC-LF NC/μ as displayed in Fig. 2. We have already shown that both behaviours, the negative tan(ϕ) and γ>1, originate from a sensitization of the material [13]. This shows again that both techniques are closely linked to the same mechanisms.

However, we have also extracted N values from the MPC-LF data, taking the first *positive* slope of the variations of tan(ϕ) vs ω, and this results in the plot of MPC-LF NC/μ displayed in Fig. 4, where the gap between the CBT and the DB states has obviously disappeared. However, there is still a discrepancy between MPC-LF and MPC-HF NC/μ, and, if we assume that the MPC-LF experiment is still giving N values, it would mean that in this region the defect density is low, according to the MPC-LF results, but its C is high enough to give the MPC-HF NC/μ values. We shall come back to this point in Section 4 where we present numerical simulation results.

In summary, the analysis of the discrepancies between the different NC/μ's extracted from several experiments, based on the different theoretical developments, leads to the knowledge of the DOS distributions, as well as some of the capture coefficients. Experimentally we can deduce:
(a) the $C_n^{CBT} N_c$ as well as the $\mu_n N_c$ values from the adjustment of the MPC-LF and MPC-HF NC/μ values in the CBT region,
(b) the DOS shape in the CBT region and close to the Fermi level, and thus the maximum value of the deep defect density N^{DB},
(c) an estimate of $C_n^{VBT} N_c$ from the ratio of the MPC-HF NC/μ and γ-NC/μ values in the CBT region,
(d) an estimate of the $C_n^{DB} N_c$ value from the ratio of the MPC-LF and MPC-HF NC/μ values at deep energies, and
(e) an order of magnitude of the ratio between the capture coefficients of charged and neutral DB states from the ratio of the MPC-HF NC/μ and γ-NC/μ values at deep energies.

We have summarized, in Table 1, the values of the different DOS parameters that could be extracted from the data of the three experiments performed on the same film. The C and μ values have been calculated assuming that N_c=2.5×10^{19} cm^{-3} as for c-Si. This choice leads to rather high mobility values, though still reasonable [14]. A choice of N_c three times higher would have lead to the commonly quoted value of μ_n=10 cm^{2}V^{-1}s^{-1} [15], but would also give capture coefficients three times lower.

Table 1. Summary of the different DOS parameters determined from the experimental results.

803242	AD	LS	Annealed
μ_n (cm^2/V/s)	30	50	50
C_n^{CBT} (cm^{3}s^{-1})	5.0×10^{-9}	2.5×10^{-8}	1.2×10^{-8}
C_n^{VBT} (cm^{3}s^{-1})	6×10^{-10}	5×10^{-10}	7×10^{-10}
$N^{CBT}(0.25)$ (cm^{-3}eV^{-1})	3.5×10^{18}	7.2×10^{18}	6.4×10^{18}
C_n^{DB} (cm^{3}s^{-1})	1.2×10^{-9}	4.0×10^{-9}	2.4×10^{-9}
N^{DB} (cm^{-3}eV^{-1})	4×10^{17}	8×10^{17}	5×10^{17}

From the results in Table 1, we can comment on the evolution of the DOS parameters following the different treatments applied to the a-Si:H film.

There is an apparent increase in the extended state electron mobility, but we believe that this is mostly due to the uncertainty in the matching between the MPC-LF and MPC-HF results in the CBT region. A mean mobility of 40 cm^{2}V^{-1}s^{-1} probably would have also led to a good matching in all the states of the film. Hence, we can estimate that the data in Table 1 are given with an uncertainty of ~ 30%. Despite this uncertainty, it is rather apparent that light-soaking seems to result both in an increase of the density of states – both in the deep states and the CBT states – and in an increase of some of the C_n, as already reported in the literature [16-17]. It is the combination of both processes that results in a material with degraded properties. Besides this, it seems that the increase in the capture coefficients is more pronounced

than the increase in the DOS. For instance, C_n^{CBT} increases by a factor of the order of 5 whereas the CBT DOS at 0.25 eV, $N^{CBT}(0.25)$, increases by a factor of the order of 2. It can also be seen, as already shown elsewhere for many a-Si:H samples [18], that annealing does not restore the initial properties of the CBT and the deep defects, the capture coefficients remaining higher than in the AD state. Surprisingly, there is no evolution of C_n^{VBT} upon light-soaking and annealing, but this result is based on only two points obtained from γ measurements at a very high flux (see Fig. 3), so it should be taken very cautiously.

4. Numerical simulation

As seen in the previous section, it seems that from the experimental data coming from the three photoconductivity experiments, it is possible to extract a lot of information both on the density of defects and on the capture coefficients of a-Si:H films. However, there is still a point that remains unclear: the presence of a defect density in between the CBT and the DB that would account for the MPC-HF and LF results in the energy range 0.35-0.5 eV, if one takes the first positive variations of tan(ϕ) vs ω to calculate N from the MPC-LF technique. To clarify this point, and also to illustrate the DOS parameter determinations, we have used a numerical simulation. Actually, two simulations were developed, one in Argentina and one in France, with different programming languages, but both based on the theoretical developments presented in Section 1, in order to cross check the numerical results. One of these simulations is available on the internet [19]. In these simulation programs, the user can introduce parameters of a given semiconductor – such as the band gap width, extended states mobilities, equivalent densities of states at the band edges, capture coefficients, etc. – as well as gap states distributions – either monovalent, as the band tail states, or amphoteric, as for the DB. The user can also introduce 'experimental' data as for the flux, the temperature, the frequencies of the modulation, etc. Taking account the very large number of parameters involved, these simulations were not intended to reproduce carefully the experimental results, but rather to understand the processes involved in each of the experiments. For each 'experiment' the continuity and charge neutrality equations are numerically solved, taking account of the 'experimental' conditions, and the resulting data are treated afterwards as we have proceeded with true experimental data. Most of the orders of magnitude of the parameters that we have introduced in the simulations come either from our experimental results or from the literature.

We present in Fig. 5 the density of states as well as the capture coefficients of the different distributions introduced in the simulation, to try to reproduce the results obtained on the AD or ANN states. The gap width was fixed at 1.8 eV. To obtain almost the same NC/μ distribution in the CBT region as the experimental one, the CBT was made of two exponential distributions; the deeper part representing a characteristic temperature of T_c = 275 K and the upper part a T_c = 440 K. For the VBT distribution, we have also used two exponential distributions, with a characteristic temperature of T_v = 600 K (as for device grade material [20]) for the deeper part, and T_v = 780 K for the shallowest part of the tail. In both cases, the band tails reach a maximum value of 10^{21} cm^{-3}eV^{-1} at the band edges. The reader may note that these shapes correspond to previous results obtained from time of flight measurements [14, 21]. The capture coefficients were all taken to be equal to 10^{-8} cm^{3}s^{-1}, except C_n^{VBT} that was chosen to be 10 times lower. These values corresponding, to within an order of magnitude, to the data displayed in Table 1.

Deep defects, corresponding to DB states, have been introduced following the defect pool model described by Powell and Deane [12]. Of course, the proper statistics for amphoteric states was used and taken into account, both in the continuity and charge neutrality equations. In the simulation, we have used a pool position of E_c-E=0.72 eV, a standard deviation of 0.11 eV, a hydrogen concentration of 5×10^{21} cm^{-3}, and a correlation energy of 0.15 eV. These parameters set the dark Fermi level at 0.755 eV and gave a total concentration of neutral DB of 2.5×10^{16} cm^{-3} [20]. The capture coefficients were taken equal to C_n^0=1.5×10^{-9} cm^{3}s^{-1} and C_p^0=3.0×10^{-9} cm^{3}s^{-1}, with ratios of 1 for C_n^+ ($C_n^+ = C_n^0$) and 10 for C_p^- (C_p^-=10× C_p^0).

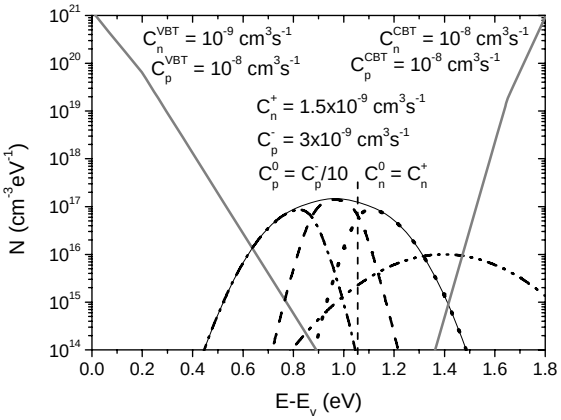

Fig. 5. DOS distributions and their capture coefficients introduced in the simulation. A defect pool model has been used to defined the DB's whose three states of charge are shown: D^+ with dotted line, D^0 in dashed line and D^- in dash dotted line. Additional acceptor states are presented in a dash-dot-dotted line.

As we suspect, the presence of an additional density of states in between the CBT and the DB distribution, we have added Gaussian shape acceptor states peaked at 0.4 eV below E_c, with a maximum value of 10^{16} cm^{-3}eV^{-1} and a standard deviation of 0.2 eV. The capture coefficients were fixed at C_n=10^{-7} (i.e. rather high) and C_p=10^{-8} cm^{-3}eV^{-1}.

The extended state mobilities were taken equal to μ_n=10 $cm^2V^{-1}s^{-1}$ and μ_p=1 $cm^2V^{-1}s^{-1}$.

The results of the simulations are displayed in Fig. 6. The analogy with the experimental behaviour is obvious (see Fig. 2 or Fig. 4). It can also be seen that if the MPC-LF data are treated taking, for the first slope of tan(ϕ) vs ω one obtains a gap in the energy range 0.35-0.45 eV, whereas taking the first positive slope of tan(ϕ) vs ω (open circles), this fills this gap with NC/μ values corresponding to the extra Gaussian distribution we have introduced between the CBT and the DB states. Thus, although this result cannot be considered as direct evidence of the presence of some extra states in the gap, it is likely that these states do exist; the question of their origin remaining unanswered.

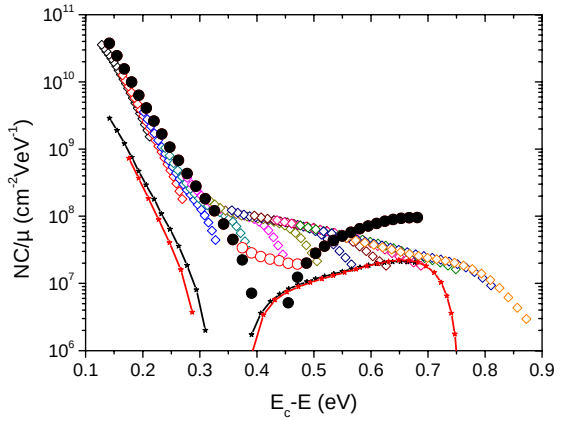

Fig. 6. Plots of the various NC/μ from the results of the numerical simulation, using the parameters of an as-deposited 'film'. The symbols are the same as for the experimental results.

Following the experimental data we have obtained after light-soaking, we have also performed a simulation in which the parameters have been modified accordingly, trying to mimic the experimental behaviours of a light-soaked film. Hence, we have increased C_n^{CBT} by a factor of five and C_n^0 by a factor of 3. Though we have experimentally found that C_n^{VBT} seemed to be constant, we have increased this parameter by a factor of 2 in the simulation, for it would be rather strange that this parameter does not evolve with light-soaking. The CBT density of states, as well as the deep defect density, were also raised by a factor of 2. The other parameters on which we have no information were kept the same. We present in Fig. 7 the results of the simulation of the MPC-LF and MPC-HF experiments. Again the analogy with the experimental results displayed in Fig. 3 is obvious.

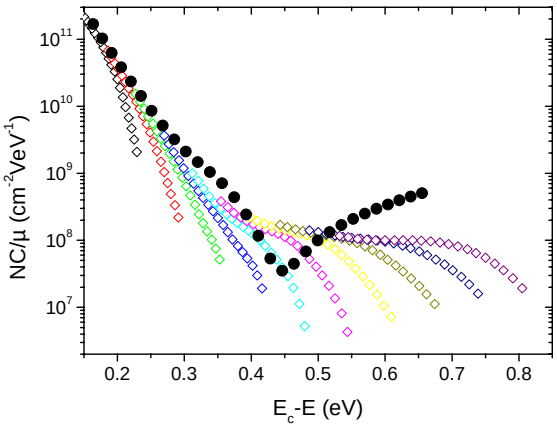

Fig. 7. Plots of the various NC/μ from the results of the numerical simulation, using the parameters of a light-soaked 'film'. The symbols are the same as for the experimental results.

5. Conclusions

From the theoretical developments of three different experiments based on the photoconductivity properties of a semiconductor, three DOS spectroscopies have been proposed. Taking advantage of the fact that these different spectroscopies are not sensitive to the same parameters, we have derived some parameters of the DOS of an a-Si:H film in the as-deposited, light-soaked and annealed states. Comparing these results, we have found that light-soaking resulted both in an increase of some capture coefficients and of the density of states.

Besides this, all the experimental behaviours have been reproduced by means of numerical simulations, in which the parameters deduced from the experiments in the as-deposited and light soaked states of the film have been introduced. From these simulations, we have also confirmed that an additional distribution of defects between the conduction band tail and the dangling bond states may exist.

Acknowledgements

Many thanks to P. Roca i Cabarrocas for supplying the polymorphous sample. J.A.S and R.R.K. acknowledge support from ANPCyT, CONICET and UNL. This work was also partly support by Ecos-Sud program A02E01.

References

[1] H. Oheda, J. Appl. Phys. **52**, 6693 (1981).
[2] K. Hattori, Y. Niwano, H. Okamoto, Y. Hamakawa, J. Non-Cryst. Solids **137&138**, 363 (1991).
[3] R. Brüggemann, C. Main, J. Berkin, S. Reynolds, Phil. Mag. B **62**, 29 (1990).

[4] C. Longeaud, J. P. Kleider, Phys. Rev. B **45**, 11672 (1992).
[5] C. Longeaud, J. A. Schmidt, J. P. Kleider, Phys. Rev. B **73**, 235316 (2006).
[6] C. Longeaud, J. A. Schmidt, R. Koropecki, Phys. Rev. B **73**, 235317 (2006).
[7] M. E. Gueunier, C. Longeaud, J. P. Kleider, Eur. Phys. J. Appl. Phys. **26**, 75 (2004).
[8] M. Q. Tran, Phil. Mag. B **72**, 35 (1995).
[9] J. Z. Liu, S. Wagner, Phys. Rev. B **39**, 11156 (1989).
[10] A. Rose, Concepts in photoconductivity and allied problems, Wiley & sons, New York (1966).
[11] P. Roca i Cabarrocas, S. Hamma, P. St'ahel, C. Longeaud, J. P. Kleider, R. Meaudre, M. Meaudre, Proc. 14-th European Photovoltaic Energy Conference and Exhibition, Ed. H. A. Ossenbrink, P. Helm, H. Ehmann (Bedford: H. S. Stephens & Associates), Barcelona, Spain, 1997, p. 1444.
[12] M. J. Powell, S. C. Deane, Phys. Rev. B **48**, 10815 (1993).
[13] J. A. Schmidt, C. Longeaud, J. Appl. Phys. **101**, 103705 (2007).
[14] R. Vanderhaghen, Phys. Rev. B **38**, 10755 (1988).
[15] T. Tiedje, in Semiconductors and Semimetals **21**C, Ed. by J. Pankove, Academic Press, pp 207-238 (1984).
[16] M. Meaudre, R. Meaudre, J. Phys. : Condens. Matter **13**, 5663 (2001).
[17] P. Kounavis, E. Mytilineou, Solid State Phenom. **44-46**, 715 (1995).
[18] C. Longeaud, D. Roy, O. Saadane, Phys. Rev. B **65**, 085206 (2002).
[19] DEOST at www.lgep.suplec.fr/scm
[20] M. Stutzmann, Philos. Mag. B **60**, 531 (1989).
[21] C. Longeaud, G. Fournet, R. Vanderhaghen, Phys. Rev. B **38**, 7493 (1988).

*Corresponding author: longeaud@lgep.supelec.fr